EPR Characterization of Photosystem II from Different Domains of the Thylakoid Membrane[†]

Fikret Mamedov,*[,‡] Ravi Danielsson,[§] Rena Gadjieva,[§,⊥] Per-Åke Albertsson,[§] and Stenbjörn Styring[‡]

Molecular Biomimetics, Department of Photochemistry and Molecular Science, Ångström Laboratory, Box 523, Uppsala University, Uppsala 75120, and Department of Biochemistry, Center for Chemistry and Chemical Engineering, Lund University, P.O. Box 124, Lund 22100, Sweden

Received September 19, 2007; Revised Manuscript Received December 21, 2007

ABSTRACT: We report electron paramagnetic resonance (EPR) studies on photosystem II (PSII) from higher plants in five different domains of the thylakoid membrane prepared by sonication and two-phase partitioning. The domains studied were the grana core, the entire grana stack, the grana margins, the stroma lamellae and the purified stromal fraction, Y100. The electron transport properties of both donor and acceptor sides of PSII such as oxygen evolution, cofactors Y_D, Q_A, the $CaMn_4$-cluster, and $Cytb_{559}$ were investigated. The PSII content was estimated on the basis of oxidized Y_D and Q_A^- Fe^{2+} signal from the acceptor side vs Chl content (100% in the grana core fraction). It was found to be about 82% in the grana, 59% in the margins, 35% in the stroma and 15% in the Y100 fraction. The most active PSII centers were found in the granal fractions as was estimated from the rates of electron transfer and the S_2 state multiline EPR signal. In the margin and stroma fractions the multiline signal was smaller (40 and 33%, respectively). The S_2 state multiline could not be induced in the Y100 fraction. In addition, the oxidized LP $Cytb_{559}$ prevailed in the stromal fractions while the HP form dominated in the grana core. The margins and entire grana fractions have $Cytb_{559}$ in both potential forms. These data together with previous analyses indicate that the sequence of activation of the PSII properties can be represented as: PSII content > oxygen evolution > reduced $Cytb_{559}$ > dimerization of PSII centers in all fractions of the thylakoid membrane with the gradual increase from stromal fractions via margin to the grana core fraction. The results further support the existence of a PSII activity gradient which reflects lateral movement and photoactivation of PSII centers in the thylakoid membrane. The possible role of the PSII redox components in this process is discussed.

Photosystem II (PSII)[1] is one of the four protein complexes embedded in the thylakoid membrane of the chloroplast (*1*). It uses light energy to extract electrons from water and to reduce the plastoquinone pool (*2–4*). PSII is a large Chl−protein complex with more than 25 subunits, although most of its electron transfer cofactors are bound to the D1/D2 protein heterodimer (*5*). Its crystal structure has been revealed at medium 3.0–3.8 Å resolution (*6–9*). The catalytic center of PSII, which includes Y_Z, a redox active tyrosine residue, and the $CaMn_4$-cluster, is the site where water oxidation occurs (*10–13*).

To oxidize water, PSII must work at high redox potentials (>1.12 V (*3*)). Because of such oxidative photochemistry PSII is vulnerable to environmental stress, and, for example, an excess of light can inhibit oxygen evolution and electron transport in PSII. These photoinhibition events further lead to degradation of the D1 protein and disassembly of PSII centers. Thereafter, these centers are reassembled using newly synthesized copies of the D1 protein (*14, 15*) leading to coordinated activation of oxygen evolution and electron transport (*16–20*). All these events are part of the photoinhibition/repair cycle of PSII, which takes place in all green plants on an everyday basis (*14, 15, 20*) and is the major reason why PSII can *always* be found in different functional and structural forms in the thylakoid membrane (for reviews see refs *20* and *21*). Different events of this cycle occur in different parts of the thylakoid membrane (*20, 24–26*). In higher plants, this membrane has a complex organization and can be differentiated into four domains (*22*): the stroma lamellae, which are single paired and exposed to the chloroplast stroma, the grana margins, which are also exposed to the stroma and form an annulus around the third domain, the stacked membranes of the grana core. The end membranes of a grana stack may constitute a fourth domain of the thylakoid membrane (*23*).

[†] This work was supported by grants from The Swedish Research Council, The Swedish Energy Administration, DESS, and The Knut and Alice Wallenberg Foundation.

* Corresponding author. Phone: +46 (0)18 471 6581; fax: +46 (0)18 471 6844; e-mail: fikret.mamedov@fotomol.uu.se.

[‡] Uppsala University.

[§] Lund University.

[⊥] Current address: Department of Forest Mycology and Pathology, Swedish University of Agricultural Sciences, Box 7026, Uppsala 75007, Sweden.

[1] Abbreviations: Chl, chlorophyll; Cyt, cytochrome; EPR, electron paramagnetic resonance; F_A and F_B, iron-sulfur clusters in PSI; F_V, variable fluorescence; F_0, initial level of fluorescence; MES, 4-morpholine ethanesulfonic acid; HP and LP, the high and low potential of $Cytb_{559}$, respectively; P680, the primary electron donor in PSII; OEC, oxygen evolving complex; Pheo, pheophytin; PpBQ, phenyl-*p*-benzoquinone; PS, photosystem; Y_D, the redox active tyrosine residue D2–161 in PSII; Y_Z, the redox active tyrosine residue D1–161 in PSII.

10.1021/bi701913k CCC: $40.75
Published on Web 02/28/2008

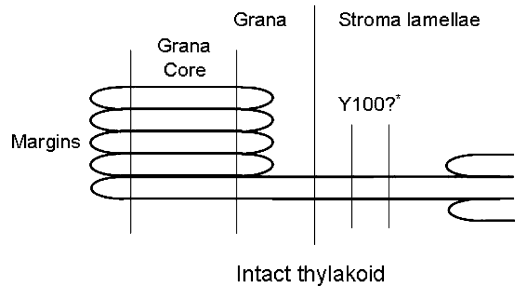

FIGURE 1: Terminology and schematic representation of the different fractions of the thylakoid membrane studied in this work. *The exact origin of the Y100 fraction within the stroma-exposed region is unknown.

The most active PSII centers are found in the grana core where dimeric forms of PSII dominate (*25*). These PSII centers have large antennae (*26*), are active in oxygen evolution, and are efficient in Q_A^- to Q_B electron transfer (*24*). The majority of the PSII centers in the thylakoid membrane are found here. In contrast, the PSII centers in the stroma lamellae are mostly in the monomeric form (*25*) with a small antenna (*26*), a varying oxygen evolving activity and slow or inefficient electron transfer from Q_A^- to Q_B (*20*). In the margins of the grana core, the PSII population is heterogeneous, and both dimeric and monomeric PSII are frequently found. In addition, the antenna and electron transfer properties are mixed, and this part of the membrane contains centers both active and inactive in oxygen evolution or electron transfer on the acceptor side (*24, 26*).

We apply a non-invasive, two-phase partitioning method without any detergent treatment to isolate five different subfractions of the thylakoid membrane (Figure 1): the grana core, the grana margins, the entire grana (grana core plus margins), the stroma lamellae, and the stroma lamellae Y100 (*22, 24–28*). This method preserves the native organization of membrane domains and allows the study of PSII in different parts of the thylakoid membrane. Previously we used steady-state electron transport and flash-induced fluorescence decay measurements to investigate the general electron transport properties of PSII. We found that these properties were different in these fractions (*24*). However, the molecular basis for these differences was not accessible, and it was clear that a more informative spectroscopical approach is required to address this problem. Moreover, specific monitoring of cofactors, involved in the water oxidation and electron transport in PSII from different fractions of the thylakoid membrane, was needed.

In this study, we have applied such an informative approach, EPR spectroscopy, to thylakoid fractions. Almost every single electron carrier in PSII can be followed independently by EPR spectroscopy. Thereby, we have been able to characterize most of the electron transport cofactors in PSII from different fractions of the thylakoid membrane. More importantly, we were able to compare our new data to our previous studies on functional and structural differences and to derive a comprehensive picture of PSII in the thylakoid membrane.

MATERIALS AND METHODS

Preparation of Thylakoid Membrane Fractions. Spinach (*Spinacia oleracia* L.) was grown hydroponically at 20 °C with a light/dark period of 12 h and a light intensity of 300 μE m^{-2} s^{-1}. The spinach leaves were dark adapted 24 h prior to isolation procedure. The light source (dysprosium lamps, Osram HQI-E400W/DV) has spectral characteristics close to daylight, and comparison with a greenhouse grown spinach showed no significant difference in the properties of isolated thylakoid fractions (*22–28* and references therein). The thylakoid membranes and five different thylakoid membrane fractions, the grana core, the grana margins, the entire grana (the grana core and grana margins), the stroma lamellae, and the Y100 fraction were prepared as described previously (see ref *28* and references therein). All fractions were resuspended in 300 mM sucrose, 15 mM NaCl, and 15 mM MES-NaOH (pH 6.5) and stored at 77 K at 3–4 mg of Chl mL^{-1}.

The oxygen evolution was measured with a Hansatech Clark-type electrode using saturating light in the resuspension buffer with a mix of 0.5 mM PpBQ and 2 mM ferricyanide as external electron acceptors.

EPR Spectroscopy. EPR measurements were performed at liquid He temperatures with a Bruker ELEXYS E500 spectrometer equipped with the SuperX ER049X microwave bridge and an ER4122SHQ cavity. The temperature was regulated with an Oxford-900 cryostat and ITC-4 temperature controller.

Samples from the different fractions, in calibrated EPR tubes, were preilluminated by room light at 293 K for 2 min to fully oxidize Y_D (which forms a stable radical in all PSII centers after this treatment (*29*)). After 5 min of dark adaptation the samples were frozen for EPR measurements. The S_2 state multiline and $g = 4.1$ signals were induced by saturating illumination at 200 K in an ethanol/dry ice bath (*30–32*). Oxidation of $Cytb_{559}$ was achieved by illumination at 77 K (*32–34*). The fraction of the HP form of $Cytb_{559}$ ($g_z = 3.06$, "frozen state", *35, 36*) was determined by subtraction of the adjusted spectrum of the LP $Cytb_{559}$ (dark adapted BBY sample, $g_z = 2.96$) from the spectrum of total $Cytb_{559}$ (recorded after illumination at 77 K). The rest of the spectrum was attributed to the LP form. The time for the illumination procedures was controlled independently for each of the samples originating from the different parts of the thylakoid membrane to achieve maximal induction of the EPR signals. Different illumination times were applied for each fraction since the antennae size of PSII varies substantially. The Q_A^- Fe^{2+} signal was induced in the presence of 50 mM of formate after reduction with 50 mM dithionite in the dark at 293 K (*34, 37*). Analysis of the spectra was performed using the Bruker Xepr 2.1 software.

RESULTS

Estimation of the PSII Content in the Different Fractions on the Basis of $Y_D^\bullet$. $Y_D^\bullet$ is stable for tens of minutes in thylakoid membranes and PSII membrane preparations (*29, 38–40*). When fully induced, this stable radical represents 1 spin per PSII reaction center and is, therefore, an accurate probe for the PSII content (*41*). As shown before by us in measurements at room temperature, (*28*) the amount of $Y_D^\bullet$ varied in the different fractions (on the basis of the Chl content, Figure 2, Table 1). The largest signal was observed in the grana core fraction and $Y_D^\bullet$ here was taken as 100% to allow comparison to the EPR signals from the other fractions. This approach was also used for the other EPR signals analyzed

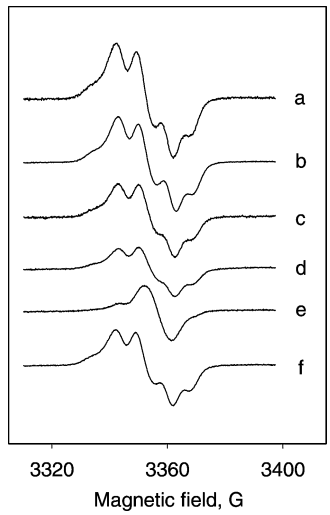

FIGURE 2: EPR spectra of $Y_D^{\bullet}$ from PSII in different fractions of the thylakoid membrane: (a) the grana core, (b) the grana, (c) the margins, (d) the stroma lamellae, (e) the Y100 fraction, and (f) the intact thylakoid membrane. The spectra were normalized to the same Chl concentration. The full induction of $Y_D^{\bullet}$ was achieved as described in Materials and Methods. Experimental conditions: microwave frequency 9.41 GHz, microwave power 1.3 μW, modulation amplitude 3.5 G, temperature 15 K.

in this work (see Table 1). In the entire grana fraction, $Y_D^{\bullet}$ was slightly higher than 80% as compared to the grana core fraction. The $Y_D^{\bullet}$ signal from the margin and stroma lamellae fractions was found to be about 60 and 35%, respectively. The Y100 fraction showed about 15% of $Y_D^{\bullet}$ (Figure 2, Table 1). Thus, there is a gradual increase of the amount of PSII centers, from the Y100 fraction through the stroma lamellae and margins to the grana core fraction. This reflects that there is more PSI in the stroma lamellae and margins, and our low temperature EPR measurements here confirm our earlier study performed at room temperature (*28*).

In the margins, the stroma lamellae and the Y100 fractions a small radical was observed on top of the $Y_D^{\bullet}$ spectrum (clearly visible in Figure 2, spectrum e). This signal has been described by us earlier and was 8.0–8.5 G wide, had a *g*-value of 2.0026, and most probably originated from $P700^+$ (*28*). The amount of this radical varied with preparation and is likely to reflect the redox conditions in the particular membrane fraction. This remaining $P700^+$ was less than 5% in the margin fraction, less than 15% for the stroma lamellae, and about 50% in the Y100 fraction as compared to the corresponding $Y_D^{\bullet}$ spectrum (Figure 2). In the Y100 fraction it involved ca. 5% of the PSI centers present here as there is more than 10 PSI centers per one PSII (*28*). Consequently, this radical represents a minor fraction of PSI present.

The Q_A^- Fe^{2+} Acceptor Side Complex in the Different Fractions of the Thylakoid Membrane. A valuable alternative spectroscopic probe for both the PSII content and the integrity of the acceptor side is the EPR signal that arises from magnetic interaction between Q_A^- and the nearby Fe^{2+} atom. The EPR signal, denoted the Q_A^- Fe^{2+} signal, is greatly enhanced in the presence of formate (*32, 37*) and can be used for quantification and analysis of PSII centers (*34, 42*). In the presence of dithionite and formate, the Q_A^- Fe^{2+} signal is characterized by a peak at $g = 1.82$ and a trough at $g = 1.69$ (*37, 43*). The signal was observable in all fractions studied (Figure 3). Our estimation of the amplitude of the Q_A^- Fe^{2+} signal is shown in Table 1.

On a Chl basis, the biggest Q_A^- Fe^{2+} signal (set to 100%) was observed in the grana core fraction. In the grana fraction, it was found to be 94% as compared to the grana core fraction. The signal from the margin and stroma lamellae fractions was about 40 and 30%, respectively. In the Y100 fraction the signal was small and was about 13% of that in the grana core (Figure 3, Table 1). It is worth mentioning that no free radical EPR signal (*44–46*) was observed from the magnetically uncoupled semiquinone radical in any of the fractions. This shows that there were no PSII centers where Q_A^- could be formed in the absence of the nearby Fe^{2+}.

Induction of the S_2 State Multiline and $g = 4.1$ Signals in the Different Fractions of the Thylakoid Membrane. In most membrane preparations containing PSII, not all of the PSII centers contribute to the oxygen evolution. The main reason is that some PSII centers have been inhibited by, for example, photoinhibition, or that photoactivation of the $CaMn_4$-cluster is not yet complete in newly assembled centers. Our estimation of the fraction of oxygen-evolving PSII centers on the basis of steady-state electron transport measurements is presented in Table 1. This measurement does not allow distinction of the site at which inhibition occurs. Therefore, we have measured the S_2 state multiline and $g = 4.1$ EPR signals, which both originate from the oxygen-evolving complex and are other useful probes to PSII centers with an active $CaMn_4$-cluster (*32, 47–49*). In addition, both EPR signals are spectroscopic probes that are known to be

Table 1: Relative Amplitudes of EPR Signals (Determined on a Chl Basis) from $Y_D^{\bullet}$, the Q_A^- Fe^{2+} Signal, the S_2-State Multiline EPR Signal from the $CaMn_4$-Cluster, and the g_z Region of Oxidized $Cytb_{559}$, Combined with General Characteristics of PSII in Different Fractions of the Thylakoid Membrane

fraction of thylakoid membrane	$Y_D^{\bullet}$[a] (%)	Q_A^- Fe^{2+}[b] (%)	F_V/F_0[c] (%)	DPC → DCIP[d] mediated electron transfer (%)	S_2 state multiline[e] (%)	O_2 evolution (%)	$Cytb_{559}$ dark/illum[f]	LP $Cytb_{559}$ (%)	HP $Cytb_{559}$ (%)
grana core	100	100	100	100	100	100	0.21	30	70
grana	82	94	87	86	92	87	0.35	21	79
margins	59	39	44	58	40	38	0.54	38	62
stroma	35	31	25	34	33	29	0.75	40	60
Y100	15	13	18	11	0	0	0.87	58	42

[a] Induced by illumination and subsequent dark adaptation at 293 K (see Materials and Methods). The remaining fraction of $P700^+$ radical was subtracted from the EPR spectra recorded for the margins, stroma lamellae and Y100 fractions prior to estimation of $Y_D^{\bullet}$ as in ref *28*. [b] Induced by chemical reduction using 50 mM dithionite in presence of 50 mM formate. [c] Estimated from the fluorescence measurements (*24*). [d] Estimated from the DCIP reduction in the presence of the exogenous electron donor DPC (*24*). [e] Induced by saturating illumination at 200 K. [f] Ratio between the fraction of initially present oxidized $Cytb_{559}$ (in the dark adapted samples) and total $Cytb_{559}$ (after oxidation by illumination at 77 K). Oxidized $Cytb_{559}$ was estimated from integration of the g_z peak; see Materials and Methods (Figure 5).

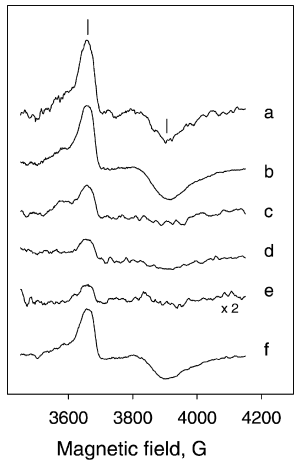

FIGURE 3: The EPR signal from the reduced Q_A^- Fe^{2+} complex in PSII from different fractions of the thylakoid membrane: (a) the grana core, (b) the grana, (c) the margins, (d) the stroma lamellae, (e) the Y100 fraction, and (f) the intact thylakoid membrane. The spectra were normalized to the same Chl concentration (spectrum e was multiplied two times). The signal was induced by chemical reduction with 50 mM dithionite in the presence of 50 mM formate. The bars indicate the spectral features at $g = 1.82$ and $g = 1.69$, which are typical for the Q_A^- Fe^{2+} signal in presence of formate. Experimental conditions: microwave frequency 9.41 GHz, microwave power 20 mW, modulation amplitude 15 G, temperature 4 K.

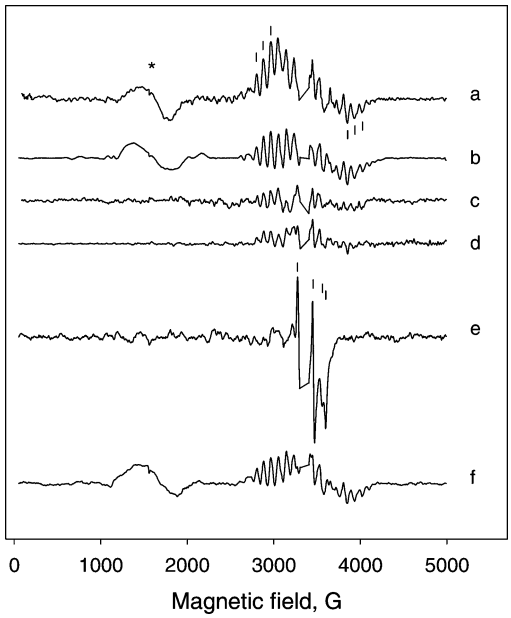

FIGURE 4: The light minus dark difference wide scan spectra showing the S_2 state multiline and $g = 4.1$ (*) signals from the oxygen-evolving complex in PSII from the different fractions of the thylakoid membrane: (a) the grana core, (b) the grana, (c) the margins, (d) the stroma lamellae, (e) the Y100 fraction, and (f) the intact thylakoid membrane. Spectra a−d were reproduced with permission from ref *25* (Copyright 2007 by CCC, Inc.). The spectra were normalized to the same Chl concentration. The S_2 state EPR signals were induced in the absence of an electron acceptor by illumination at 200 K. Illumination time was 6 min for spectra a, b, and f, 8 min for spectra c and d, and 12 min for spectrum e to ensure the maximal yield of the signals. The bars in spectrum a indicate peaks chosen for the signal quantification. The bars in spectrum e show *g* values at 2.05, 1.94, 1.88, and 1.85, characteristic for EPR spectra from the reduced F_A and F_B iron-sulfur clusters in PSI. Experimental conditions: microwave frequency 9.41 GHz, microwave power 10 mW, modulation amplitude 15 G, temperature 7 K.

extremely sensitive to small structural changes in the vicinity of the $CaMn_4$-cluster (*32, 50, 51*).

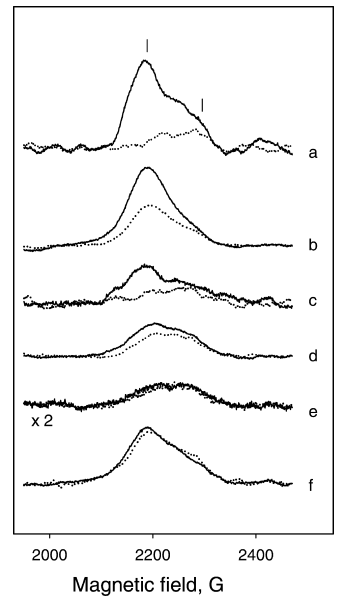

FIGURE 5: The EPR spectra from the g_z region of oxidized $Cytb_{559}$ in the dark (dotted line) and after illumination at 77 K (solid line) in PSII from different fractions of the thylakoid membrane: (a) the grana core, (b) the grana, (c) the margins, (d) the stroma lamellae, (e) the Y100 fraction, and (f) the entire thylakoid membrane. Spectra a, c−e (dotted line) were reproduced with permission from ref *25* (Copyright 2007 by CCC, Inc.). Illumination time was 8 min for spectra a−d, 12 min for spectrum e, and 6 min for spectrum f to ensure the maximal oxidation of $Cytb_{559}$. The spectra were normalized to the same Chl concentration (spectrum e was multiplied 2 times). The bars indicate the spectral features at $g = 3.06$ (left) and $g = 2.96$ (right), which are typical for the HP and the LP forms of $Cytb_{559}$, respectively. Experimental conditions: microwave frequency 9.41 GHz, microwave power 5 mW, modulation amplitude 15 G, temperature 15 K.

Figure 4 shows light minus dark difference EPR spectra that have been obtained from the different fractions of the thylakoid membrane after illumination at 200 K. Estimation of the S_2 state multiline signal size is shown in Table 1. The largest signal (on a Chl basis) was observed in the grana core fraction (set to 100%, Table 1). The entire grana fraction showed 92% of the multiline signal. In the margin and stroma lamellae fractions, the amount of inducible S_2 state multiline signal was about 40 and 30%, respectively. No multiline signal was visible in the Y100 fraction after 200 K illumination (Figure 4, Table 1) where the illumination resulted in reduction of the F_A and F_B iron-sulfur clusters in PSI, which totally dominated this fraction of the thylakoid membrane (*28*). Consequently, the EPR spectrum (Figure 4, spectrum e) was dominated by superposition of spectra from both clusters with features at $g = 2.5$, 1.94, 1.88, and 1.85 (*52–54*).

Table 1 shows that the oxygen-evolving centers in the membrane fractions determined on the basis of the S_2 state multiline signal correlated well to the oxygen evolution. In addition, the $g = 4.1$ signal (*32, 48, 49*), another signal from the S_2 state, originating from the excited-state of the $CaMn_4$-cluster, was only observable in the grana core and entire grana fractions (Figure 4, spectra a and b).

Measurements of $Cytb_{559}$ in the Different Fractions of the Thylakoid Membrane. $Cytb_{559}$ exists in several potential forms, with the HP form dominating active PSII centers and the LP forms dominating PSII which is non-functional or damaged (*55, 56*). Therefore, we characterized the redox state of $Cytb_{559}$ in the different fractions of the thylakoid mem-

Table 2: Correlation between Different Measurements on Content, Oxygen Evolving Activity, and Structural Properties of PSII from Different Fractions of the Thylakoid Membrane

fraction of thylakoid membrane	PSII content[a] $Y_D^{\bullet}/Q_A^- Fe^{2+}$ /F_v/DPC → DCIP	O_2 evolving centers[b] H_2O → PpBQ/S_2 multiline	$g = 4.1$ signal/ PSII supercomplexes[c]	dark oxidized $Cytb_{559}$/PSII monomers[d]
grana core	1.0	1.0	present	0.7
grana	0.9 ± 0.1	0.9	present	0.9
margins	1.2 ± 0.2	0.9	absent	1.0
stroma	1.1 ± 0.2	0.9	absent	0.9
Y100	1.2 ± 0.3	0	absent	1.1

[a] Correlation between the PSII content was made by comparison of data from Table 1 (calculated as average sum of comparisons of $Y_D^{\bullet}$ content (column 2) to $Q_A^- Fe^{2+}$ signal (column 3), F_V/F_0 ratio (column 4) and overall PSII electron transfer measurements (column 5)). [b] Correlation between the oxygen evolution capability was made by comparison of data from Table 1 (S_2 state multiline EPR signal (column 6) and oxygen evolution (column 7)). [c] Correlation between induction of the $g = 4.1$ signal (Figure 4) and the presence of PSII supercomplexes in respective fractions (*25*). [d] Correlation between the fraction of oxidized in the dark $Cytb_{559}$ (Table 1, column 8) and the amount of PSII monomers in respective fractions (*25*).

brane. It is difficult to perform optical titrations of $Cytb_{559}$ in our preparations due to large spectral overlap from the $Cytb_6f$ complex in some fractions (*57, 58*). Instead, we used EPR spectroscopy where the g_z peak of the oxidized $Cytb_{559}$ is free of spectral contributions from other components. In PSII enriched membranes from higher plants (BBY-type), EPR spectra from dark adapted samples exhibit peak at $g = 2.96$, which is representative of the oxidized form of LP $Cytb_{559}$ (*35, 36, 42*). It usually constitutes about 25–30% of total $Cytb_{559}$. The HP form of $Cytb_{559}$ can be oxidized by illumination at 77 K and then gives rise to an EPR spectrum with a peak at $g = 3.06$. After illumination, the spectrum, representing the total amount of $Cytb_{559}$, consequently contains both oxidized forms of $Cytb_{559}$ (LP and HP forms *35, 36, 59*).

In our membrane fractions, the picture was more complicated since the amount of the LP and HP forms did not correspond to the amount of oxidized $Cytb_{559}$ in the dark and during illumination at 77 K, respectively. Therefore, we have used the pure LP form (spectrum from the dark adapted BBY preparation) to separate the LP and HP forms in $Cytb_{559}$ spectra from thylakoid fractions as described in Materials and Methods.

The results of our EPR measurements of $Cytb_{559}$ are presented in Figure 5 and Table 1. We compare the amounts of the oxidized and reduced forms of $Cytb_{559}$ in the dark adapted samples, and we report the fraction of the LP form vs the HP form after the deconvolution. In the dark adapted samples from the grana core fraction, 21% of $Cytb_{559}$ was in the oxidized form. The LP form involved ca. 30% of $Cytb_{559}$ (Table 1, columns 8 and 9), which indicates that about 10% of the LP form was reduced in the dark in this fraction. In the entire grana fraction 35% of $Cytb_{559}$ was oxidized in the dark and represented both the LP and HP forms as judged from Figure 5, spectrum b). Illumination at 77 K revealed that about 20% of $Cytb_{559}$ was in the LP form, while the rest was in the HP form in this fraction (Table 1). Some of the HP form (15%) was already oxidized, and some of the LP form (5%) was reduced in the dark adapted samples from this fraction (Figure 5, spectra b). In the margin fraction more than half of $Cytb_{559}$ was oxidized in the dark (54%), and about 40% was in the LP form (Table 1). Low temperature illumination mostly induced the HP form (about 60% of total $Cytb_{559}$), although slight oxidation of the LP form was also observable (Figure 5, spectra c).

In the stroma lamellae 75% of the total $Cytb_{559}$ was oxidized in the dark. About 40% was in the LP form, and ~60% was in the HP form. Illumination at 77 K resulted in oxidation of mainly HP $Cytb_{559}$ (Figure 5, spectra d). In the Y100 fraction almost 90% of $Cytb_{559}$ was already oxidized in the dark with ~60% being in the LP form (Figure 5, spectra e, Table 1). Thus, both the fraction of oxidized $Cytb_{559}$ in the dark adapted samples and the fraction of the LP form were found to increase from the apressed regions of the grana core to the nonapressed regions of the stroma lamellae.

DISCUSSION

Comparison of Data Obtained by Different Assays. Our goal in this study is to obtain a deeper, molecular understanding of the functional differences in PSII from different parts of the thylakoid membrane. To do this we combined and correlated different sets of data including our previously published results (*24–26, 28*). First, we compare the measurements that define the PSII content in the different fractions. These measurements include (i) overall steady-state electron transfer measured as reduction of DCIP and include both active, oxygen evolving PSII centers and PSII centers without the $CaMn_4$-cluster able to perform Y_Z to Q_A electron transport (with DPC as electron donor); (ii) variable fluorescence measurements that represent overall PSII activity. Two other assays are EPR measurements on PSII redox components which are integral parts of the assembled reaction center. These include (iii) the $Y_D^{\bullet}$ radical and (iv) the $Q_A^- Fe^{2+}$ signal. The data are presented in Table 1, and their correlation is summarized in Table 2 and Figure 6.

The overall electron transfer (Table 1, column 5) is almost identical to the $Y_D^{\bullet}$ content (column 2), and very similar to the F_V/F_0 ratio (column 4). Estimation, based on the $Q_A^- Fe^{2+}$ signal measurements, was also quite similar (Table 1, column 3). This correlation is shown in Table 2 and indicates the gradual decrease of PSII content in the thylakoid fractions from grana core via margins to the stroma lamellae. One exception was measurements related to the Q_A^- content, F_V/F_0 ratio and especially the $Q_A^- Fe^{2+}$ signal, in the margin fraction which were found to be somehow lower if compared to the DCIP reduction and $Y_D^{\bullet}$ measurements (Table 1) and will be discussed below.

The second comparison we made was estimation of the oxygen evolution (Table 1, column 7) and the S_2 state multiline measurements (column 6). These two measurements also followed each other in every fraction of the thylakoid membrane we studied (Table 2). Interesting

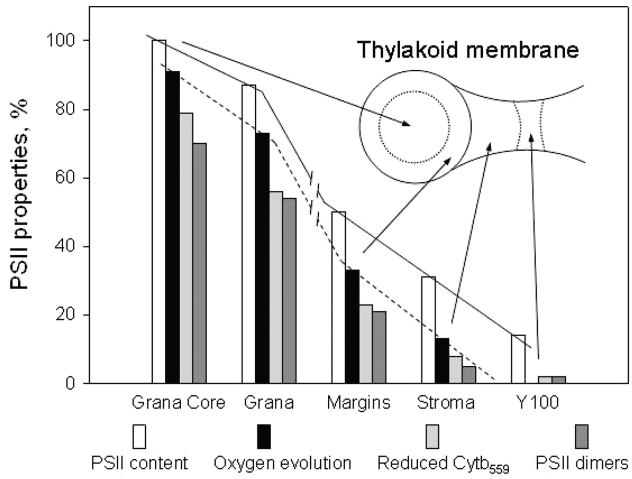

FIGURE 6: Distribution of PSII properties in the different fractions of the thylakoid membrane. White bars, average PSII content from measurements of $Y_D^{\bullet}$ and $Q_A^- Fe^{2+}$ EPR signals, F_V/F_0 ratio and overall PSII electron transfer (DPC → DCIP) from Table 1; black bars, number of oxygen evolving centers from ref *24*; light grey bars, reduced in the dark $Cytb_{559}$ from Table 1; dark grey bars, total amount of PSII dimers from ref *25*. All values were normalized to PSII content in the grana core fraction, which was set to 100%.

observations could also be made if we compare the induction of the $g = 4.1$ signal (Figure 4) with supramolecular composition of PSII in the different fractions of the thylakoid membrane (*25*) (Table 2). The induction of this signal was only possible in the granal fractions with a substantial amount of PSII supercomplexes (PSII dimer associated with several light harvesting complexes II, *25, 60*). It is known that the induction of the $g = 4.1$ signal is sensitive to treatments that can affect the overall structure of PSII (*61*). It is therefore likely that the special arrangement of PSII in the large supercomplexes somehow affects the magnetic properties of the $CaMn_4$-cluster, inducing the conditions where the $g = 4.1$ signal can be observed. This is unlikely to involve the direct interaction between the two $CaMn_4$-clusters present in the dimeric PSII complex. Instead, minor changes in the close environment of the oxygen evolving complex must be induced by supercomplex formation. It is also indicative that only the fully active PSII centers in the supercomplexes are able to induce the $g = 4.1$ signal by our illumination protocol.

The last correlation we observed in our analysis of properties of PSII from different domains of the thylakoid membrane was that the oxidation state of $Cytb_{559}$ also reflects the composition of PSII in the different fractions. Analysis of the data in Table 1 reveals that the fraction of oxidized $Cytb_{559}$ closely follows the total amount of PSII monomers in each fraction (*25*). This indicates that, most probably, preoxidized in the dark $Cytb_{559}$ can only be found in monomeric PSII complexes (Table 2). Interestingly, this oxidized fraction contains both the low and the high potential forms of $Cytb_{559}$, as revealed from analysis of the *g*-values in the EPR spectra (Figure 5) (*35*). Oxidation of $Cytb_{559}$, which is not a part of linear electron transfer events leading to water splitting, indicates necessity for electron donation in PSII (*20, 62*). Since PSII monomers are functionally heterogeneous, this implies that even oxygen evolving monomers may require alternative electron donation, especially in the nonappressed parts of membrane. Consequently, the total amount of the dimeric form of PSII in each fraction is correlated to the amount of reduced $Cytb_{559}$, which mostly contained the HP form (Tables 1 and 2, Figure 6).

Our comparison between different functional and structural properties of PSII from different domains of the thylakoid membrane is summarized in Figure 6. PSII content gradually decreased from the grana core to the stroma lamellae and Y100 fraction. This phenomenon is also ascribable to the fraction of the oxygen evolving centers in each part of the membrane. It is noticeable that the "gap" between PSII content and fraction of the fully active centers increasing from the appressed to the nonappressed regions of membrane (Figure 6). There seems to be a "breaking point" between these two types of membrane with respect to PSII properties, probably indicating that the margin fraction is an important place for PSII repair/activation cycle (Figure 6).

Functional Properties of PSII from Different Domains of the Thylakoid Membrane. By collecting our previous data on the PSII activity and composition (*20, 24–26, 28*) and data presented in this study we can define PSII in the different domains of the thylakoid membrane. We start our description with the analysis of the Y100 fraction which contains the smallest amount of PSII centers (PSI/PSII ratio is more than 10, (*28*)). This is corroborated by a clearly visible EPR signals from iron-sulfur clusters from PSI (Figure 4, spectrum e). We found that there was about 15% of PSII on the basis of $Y_D^{\bullet}$ and $Q_A^- Fe^{2+}$ measurements as compared to the grana core fraction (Table 1, Figure 6). Most of these PSII centers (~80%) are in the monomeric form (Figure 6) and 12% are found in the form of PSII reaction centers which consist of D1, D2, and $Cytb_{559}$ subunits (*25*). No oxygen-evolving centers were found in this region of the thylakoid membrane, which is reflected by the lack of the EPR signals from the $CaMn_4$-cluster (Figure 5). This is in agreement with our earlier flash-induced fluorescence measurements (*24*) that indicated that no Mn oxidation could occur. However, our measurements suggest that all centers showing $Y_D^{\bullet}$ had an active Q_A acceptor. From the similar shape of the $Q_A^- Fe^{2+}$ EPR signal in Y100 and all other fractions it also seems that Q_A and Fe^{2+} are bound to their correct environment despite lacking oxygen evolution. In our earlier fluorescence study (*24*) we found that no forward electron transfer from Q_A^- could take place. We conclude that this reflects a nonfunctional Q_B-site rather than damage to Q_A. Thus, we can conclude that PSII centers in the Y100 fraction are able to perform charge stabilization between $Y_Z^{\bullet}$ and Q_A^-.

Almost 90% of the available $Cytb_{559}$ was oxidized already before illumination in the Y100 fraction, and more than half of this was present in the LP forms. In the absence of the $CaMn_4$-cluster PSII is particularly vulnerable to photoinhibition (donor side-induced photoinhibition is a high quantum yield process (*63*)). This substantial amount of oxidized $Cytb_{559}$ indicates that it is crucial for such undeveloped PSII centers to have available an alternative donor in order to avoid photoinhibition (*20, 62, 64*).

In the stroma lamellae fraction, the amount of PSII centers is larger than in the Y100 fraction, but there are still more than three PSI centers per one PSII (*28*). We found 30–35% of $Y_D^{\bullet}$ and $Q_A^- Fe^{2+}$ signals as compared to the grana core fraction. The amount of monomeric PSII centers was essentially the same as in the Y100 fraction, although the number of reaction centers was smaller (*25*). These centers were able to perform the electron transfer from Y_Z to Q_A.

Moreover, about 40% of these PSII centers were able to perform fast electron transfer beyond Q_A^-, that is, to reduce Q_B on the microsecond time scale. About the same amount of the PSII centers contained photo-oxidizable Mn as shown by fluorescence decay measurements (*24*). This is also corroborated by oxygen evolution and S_2 state multiline EPR signal formation which was about 30% in this fraction (Table 1, Figure 4). Therefore, we can conclude that in the stroma lamellae fraction a significant amount of PSII centers was able to perform S state turnover. In addition, although there was quite a high fraction of the dark oxidized $Cytb_{559}$, the HP form was more dominant than in the Y100 fraction (60%). A small fraction of the HP form (less than 25%) was reduced in the dark, which is also indicative of those PSII centers where the oxygen-evolving complex was photoactivated (Tables 1 and 2, (*18, 24*)).

The situation in the margin fraction was somehow more complicated. The PSII/PSI ratio is close to one in this fraction (*28*). With respect to the number of PSII centers, $Y_D^{\bullet}$ measurements as well as overall electron transfer and fluorescence measurements indicated presence of about 60% of the centers, as compared to the grana core fraction (Table 1). However, our estimation of the Q_A content in this fraction, on the basis of Q_A^- Fe^{2+} signal measurements, was lower (about 40%, Table 1). This estimation is supported by variable fluorescence measurement (44% in this fraction, Table 1). It is known that variable fluorescence originates from PSII centers where Q_A is also reduced (*65*). Thus, both measurements indicate lower Q_A content in the margin fraction measured by either chemical or light reduction of Q_A. There could be two reasons for this: one is a different redox configuration of Q_A, plastoquinone pool or the whole acceptor side in 15–20% of PSII in the margin fraction. It is more likely, however, that assembly of PSII centers takes place faster than activation of the acceptor side. As we mentioned above, the margin region is an important part of the thylakoid membrane with respect to activation of PSII (*20, 24*) and also where probably disassembly of photoinhibited centers takes place (*14, 15*). This high concentration of redox events could lead to such discrepancy (*18–20, 66*).

However, the substantial amount (about 40% of PSII centers) was found in the dimeric form in the margin fraction (Figure 6 (*25*)). These PSII dimers are able to evolve oxygen and to perform S state turnover as seen from the multiline signal induction (Table 1). In addition, more reduced HP form of $Cytb_{559}$ become available as an alternative donor in this fraction (Figure 5, Table 1).

In the granal fractions the number of PSII centers reaches a maximum, and most of the centers are active in water splitting (Table 1, Figure 6). The entire grana fraction is very similar in this sense to the grana core preparation with some decrease in the PSII properties because this fraction also contains the margin region (Figure 1). Therefore, we will discuss the grana core fraction as a better representative of the apressed regions of the thylakoid membrane. The amount of PSII centers reaches a maximum and four PSII per one PSI center are found here (*28*). Most of these PSII centers (70%) are dimers and 45% have a fully developed antenna system (PSII supercomplexes (*25*)). All PSII centers have an active acceptor side complex with efficient electron transfer between quinones (*24*). About 90% of the PSII centers in the grana core are active in the oxygen evolution. The $g = 4.1$ signal from the S_2 state of the oxygen-evolving complex can be observed, which is indicative of the fully assembled, functional $CaMn_4$-cluster. It is interesting to note that the $g = 4.1$ signal was observed only in thylakoid fractions with substantial amount of PSII supercomplexes (the entire grana and the grana core preparations).

Thus, our EPR measurements of redox components in PSII from different domains, in combination with our previous data, reveal lateral PSII activity distribution. In our opinion, it is appropriate to expect that this distribution reflects a dynamic picture of PSII in the thylakoid membrane. The sequence of activation of the PSII properties can be represented as PSII content > oxygen evolution > reduced $Cytb_{559}$ > dimerization of PSII centers in all parts of the thylakoid membrane (Figure 6), and they are changing most probably concomitantly with lateral migration of the developing PSII centers from the stromal part (Y100) to the granal part of the membrane (the grana core). This occurs in combination with activation of the acceptor side and the $CaMn_4$-cluster. $Cytb_{559}$ plays an important role in preventing inhibition of PSII in the earlier stages of this process.

REFERENCES

1. Wydrzynski, T. J., and Satoh, K. (2005) *Photosystem II: the Light Driven Water: Plastoquinone Oxidoreductase*, Springer, Dordrecht, the Netherlands.
2. Barber, J. (2002) Photosystem II: a multisubunit membrane protein that oxidises water. *Cur. Opin. Struct. Biol. 12*, 523–530.
3. Diner, B. A., and Rappaport, F. (2002) Structure, dynamics, and energetics of the primary photochemistry of photosystem II of oxygenic photosynthesis. *Ann. Rev. Plant Biol. 53*, 551–580.
4. Goussias, C., Boussac, A., and Rutherford, A. W. (2002) Photosystem II and photosynthetic oxidation of water: an overview. *Philos. Trans. R. Soc. London, Ser. B 357*, 1369–1381.
5. Hankamer, B., Barber, J., and Boekema, E. J. (1997) Structure and membrane organization of Photosystem II from green plants. *Ann. Rev. Plant Physiol. Plant Mol. Biol. 48*, 641–672.
6. Zouni, A., Witt, H. T., Kern, J., Fromme, P., Krauss, N., Saenger, W., and Orth, P. (2001) Crystal structure of photosystem II from *Synechococcus elongatus* at 3.8 Å resolution. *Nature 409*, 739–743.
7. Kamiya, N., and Shen, J. R. (2003) Crystal structure of oxygen-evolving photosystem II from *Thermosynechococcus vulcanus* at 3.7-Å resolution. *Proc. Natl. Acad. Sci. U. S. A. 100*, 98–103.
8. Ferreira, K. N., Iverson, T. M., Maghlaoui, K., Barber, J., and Iwata, S. (2004) Architecture of the photosynthetic oxygen-evolving center. *Science 303* 1831–1838.
9. Loll, B., Kern, J., Saenger, W., Zouni, A., and Biesiadka, J. (2005) Towards complete cofactor arrangement in the 3.0 Å resolution structure of photosystem II. *Nature 438*, 1040–1044.
10. Renger, G. (2004) Coupling of electron and proton transfer in oxidative water cleavage in photosynthesis. *Biochim. Biophys. Acta 1655*, 195–204.
11. McEvoy, J. P., and Brudvig, G. W. (2006) Water-splitting chemistry in Photosystem II. *Chem. Rev. 106*, 4455–4483.
12. Clausen, J., and Junge, W. (2004) Detection of an intermediate of photosynthetic water oxidation. *Nature 430*, 480–483.
13. Haumann, M., Liebisch, P., Muller, C., Barra, M., Grabolle, M., and Dau, H. (2005) Photosynthetic O_2 formation tracked by time-resolved X-ray experiments. *Science 310*, 1019–1021.
14. Aro, E.-M., Virgin, I., and Andersson, B. (1993) Photoinhibition of photosystem II. Inactivation, protein damage and turnover. *Biochim. Biophys. Acta 1143*, 113–134.
15. Andersson, B., and Aro, E.-M. (2001) Photodamage and D1 protein turnover in photosystem II, in *Regulation of Photosynthesis* (Aro, E.-M., and Andersson, B., Eds.) pp 377–393, Kluwer Academic Publishers, Dorrecht/Boston/London.
16. Ananyev, G. M., Zaltsman, L., Vasko, C., and Dismukes, G. C. (2001) The inorganic biochemistry of photosynthetic oxygen evolution/water oxidation. *Biochim. Biophys. Acta 1503*, 52–68.

17. Ono, T.-A. (2001) Metallo-radical hypothesis for photoassembly of $(Mn)_4$-cluster of photosynthetic oxygen evolving complex. *Biochim. Biophys. Acta 1503*, 40–51.
18. Rova, M., Mamedov, F., Magnuson, A., Fredriksson, P.-O., and Styring, S. (1998) Coupled activation of the donor and the acceptor side of photosystem II during photoactivation of the oxygen evolving cluster. *Biochemistry 37*, 11039–11045.
19. Rova, E. M., McEwen, B., Fredriksson, P. O., and Styring, S. (1996) Photoactivation and photoinhibition are competing in a mutant of *Chlamydomonas reinhardtii* lacking the 23-kDa extrinsic subunit of photosystem II. *J. Biol. Chem. 271*, 28918–28924.
20. Mamedov, F., and Styring, S. (2003) Logistics in the life cycle of photosystem II - lateral movement in the thylakoid membrane and activation of electron transfer. *Physiol. Plant. 119*, 328–336.
21. Lavergne, J., and Briantais, J.-M. (1996) Photosystem II heterogeneity, in *Oxygenic Photosynthesis: The Light Reactions* (Ort, D. R., and Yocum, C. F., Eds.) pp 265–287, Kluwer Academic Publishers, Dordrecht/Boston/London.
22. Albertsson, P.-Å. (2001) A quantitative model of the domain structure of the photosynthetic membrane. *Trends Plant Sci. 6*, 349–354.
23. Gadjieva, R., Mamedov, F., and Albertsson, P.-Å. (1999) Fractionation of the thylakoid membranes from tobacco. A tentative isolation of 'end membrane' and purified stroma lamellae membranes. *Biochim. Biophys. Acta 1411*, 92–100.
24. Mamedov, F., Stefansson, H., Albertsson, P.-Å., and Styring, S. (2000) Photosystem II in different parts of the thylakoid membrane: a functional comparison between different domains. *Biochemistry 39*, 10478–10486.
25. Danielsson, R., Suorsa, M., Paakarinen, V., Albertsson, P.-Å., Styring, S., Aro, E.-M., and Mamedov, F. (2006) Dimeric and monomeric organization of photosytem II. Distribution of five distinct complexes in the different domains of the thylakoid membrane. *J. Biol. Chem. 281*, 14241–14249.
26. Veerman, J., McConnell, M. D., Vasil'ev, S., Mamedov, F., Styring, S., and Bruce, D. (2007) Functional heterogeneity of photosystem II in domain specific regions of the thylakoid membrane of spinach (*Spinacia oleracea* L.). *Biochemistry 46*, 3443–3453.
27. Albertsson, P.-Å., Andreasson, E., Stefansson, H., and Wollenberger, L. (1994) Fractionation of the thylakoid membrane. *Methods Enzymol. 228*, 469–482.
28. Danielsson, R., Albertsson, P.-Å., Mamedov, F., and Styring, S. (2004) Quantification of photosystem I and II in different parts of the thylakoid membrane from spinach. *Biochim. Biophys. Acta 1608*, 53–61.
29. Babcock, G. T., and Sauer, K. (1973) Electron paramagnetic resonance signal II in spinach chloroplasts. 1. Kinetic analysis for untreated chloroplasts. *Biochim. Biophys. Acta 325*, 483–503.
30. Brudvig, G. W., Casey, J. L., and Sauer, K. (1983) The effect of temperature on the formation and decay of the multiline EPR signal species associated with photosynthetic oxygen evolution. *Biochim. Biophys. Acta 723*, 366–371.
31. Zheng, M., and Dismukes, G. C. (1996) Orbital configuration of the valence electrons, ligand field symmetry and manganese oxidation states of the photosynthetic water oxidizing complex: analysis of the S_2 state multiline EPR signals. *Inorg. Chem. 35*, 3307–3319.
32. Miller, A.-F., and Brudvig, G. W. (1991) A guide to electron paramagnetic resonance spectroscopy of photosystem II membranes. *Biochim. Biophys. Acta 1056*, 1–18.
33. de Paula, J. C., Innes, J. B., and Brudvig, G. W. (1985) Electron transfer in photosystem II at cryogenic temperatures. *Biochemistry 24*, 8114–8120.
34. Styring, S., Virgin, I., Ehrenberg, A., and Andersson, B. (1990) Strong light photoinhibition of electron transport in photosystem II. Impairment of the function of the first quinone acceptor, Q_A. *Biochim. Biophys. Acta 1015*, 269–278.
35. Thompson, L. K., Miller, A.-F., Buser, C. A., de Paula, J. C., and Brudvig, G. W. (1989) Characterization of multiple forms if cytochrome b_{559} in photosystem II. *Biochemistry 28*, 8048–8056.
36. Stewart, D. H., and Brudvig, G. W. (1998) Cytochrome b559 of photosystem II. *Biochim. Biophys. Acta 1367*, 63–87.
37. Vermaas, W. F. J., and Rutherford, A. W. (1984) EPR measurements on the effects of bicarbonate and triazine resistance on the acceptor side of Photosystem II. *FEBS Lett. 175*, 243–248.
38. Rutherford, A. W., Boussac, A., and Faller, P. (2004) The stable tyrosyl radical in photosystem II: why D? *Biochim. Biophys. Acta 1655*, 222–230.
39. Vass, I., Deák, Z., Jegerschöld, C., and Styring, S. (1990) The accessory electron donor tyrosine-D of photosystem II is slowly reduced in the dark during low-temperature storage of isolated thylakoids. *Biochim. Biophys. Acta 1018*, 41–46.
40. Feyziyev, Y., van Rotterdam, B. J., Bernat, G., and Styring, S. (2003) Electron transfer from cytochrome b559 and tyrosine D to the S_2 and S_3 states of the water oxidizing complex in photosystem II. *Chem. Phys. 294*, 415–431.
41. Babcock, G. T., Blankenship, R. E., and Sauer, K. (1976) Reaction kinetics for positive charge accumulation on the water side of chloroplast photosystem II. *FEBS Lett. 61*, 286–289.
42. Mamedov, F., Rintamäki, E., Aro, E.-M., Andersson, B., and Styring, S. (2002) Influence of protein phosphorylation on the electron-transport properties of photosystem II. *Photosynth. Res. 74*, 61–72.
43. Nugent, J. H. A., Diner, B. A., and Evans, M. C. W. (1981) Direct detection of the electron acceptor of photosystem II. Evidence that Q is an iron-quinone complex. *FEBS Lett. 124*, 241–244.
44. Klimov, V. V., Dolan, E., Shaw, E. R., and Ke, B. (1980) Interaction between the intermediary electron acceptor (pheophytin) and a possible plastoquinone-iron complex in photosystem II reaction centers. *Proc. Natl. Acad. Sci. U. S. A. 77*, 7227–7231.
45. Sanakis, Y., Petrouleas, V., and Diner, B. A. (1994) Cyanide binding at the non-heme Fe^{2+} of the iron-quinone complex of photosystem II: at high concentrations, cyanide converts the Fe^{2+} from high ($S = 2$) to low ($S = 0$) spin. *Biochemistry 33*, 9922–9928.
46. Geijer, P., Peterson, S., Härndahl, U., Styring, S., and Sundby, C. (1998) Simultaneous detection of spin coupled and decoupled QA-EPR signals in photosystem II complexes isolated with isoelectric focusing. *Photosynth. Res. 58*, 231–243.
47. Dismukes, G. C., and Siderer, Y. (1981) Intermediates of a polynuclear manganese center involved in photosynthetic oxidation of water. *Proc. Natl. Acad. Sci. U. S. A. 78*, 274–278.
48. Casey, J. L., and Sauer, K. (1984) EPR detection of a cryogenically photogenerated intermediate in photosynthetic oxygen evolution. *Biochim. Biophys. Acta 767*, 21–28.
49. Zimmermann, J.-L., and Rutherford, A. W. (1986) Electron paramagnetic resonance properties of the S_2 state of the oxygen evolving complex of photosystem II. *Biochemistry 25*, 4609–4615.
50. Debus, R. J. (1992) The manganese and calcium ions of photosynthetic oxygen evolution. *Biochim. Biophys. Acta 1102*, 269–352.
51. Britt, D. R. (1996) Oxygen Evolution, in *Oxygenic Photosynthesis: The Light Reactions* (Ort, D. R., and Yocum, C. F., Eds.) pp 137–164, Kluwer Academic Publishers, Dordrecht, The Netherlands.
52. Malkin, R., and Bearden, A. J. (1978) *Biochim. Biophys. Acta 505*, 147–181.
53. Golbeck, J. H. (1999) A comparative analysis of the spin state distribution of in vitro and in vivo mutants of PsaC. *Photosynth. Res. 61*, 107–144.
54. Vassiliev, I. R., Antonkine, M. L., and Golbeck, J. H. (2001) Iron-sulfur clusters in type I reaction centers. *Biochim. Biophys. Acta 1507*, 139–160.
55. Gadjieva, R., Mamedov, F., Renger, G., and Styring, S. (1999) Interconversion of low- and high-potential forms of cytochrome b_{559} in tris-washed photosystem II membranes under aerobic and anaerobic conditions. *Biochemistry 38*, 10578–10584.
56. Mamedov, F., Gadjieva, R., and Styring, S. (2007) Oxygen-induced changes in the redox state of the cytochrome b_{559} in photosystem II depend on the integrity of the Mn cluster. *Physiol. Plant. 119*, 328–336.
57. Romanowska, E., and Albertsson, P.-Å. (1994) Isolation and characterization of the cytochrome bf complex from whole thylakoid, grana, and stroma lamellae vesicles from spinach chloroplasts. *Plant Cell Physiol. 35*, 557–568.
58. Albertsson, P.-Å., Andreasson, E., Svensson, P., and Yu, S.-G. (1991) Localization of cytochrome *f* in the thylakoid membrane: evidence for multiple domains. *Biochim. Biophys. Acta 1098*, 90–94.
59. Buser, C. A., Diner, B. A., and Brudvig, G. W. (1992) Photooxidation of cytochrome b559 in oxygen evolving photosystem II. *Biochemistry 31*, 11449–11459.
60. Dekker, J. P., and Boekema, E. J. (2004) Supramolecular organization of thylakoid membrane proteins in green plants. *Biochim. Biophys. Acta 1706*, 12–39.
61. Boussac, A., and Rutherford, A. W. (2000) Comparative study of the $g = 4.1$ EPR signals in the S_2 state of photosystem II. *Biochim. Biophys. Acta 1457*, 145–156.

62. Magnuson, A., Rova, M., Mamedov, F., Fredriksson, P.-O., and Styring, S. (1999) The role of cytochrome b_{559} and tyrosine D in protection against photoinhibition during *in vivo* photoactivation of Photosystem II. *Biochim. Biophys. Acta 1411*, 180–191.
63. Eckert, H.-J., Geiken, B., Bernarding, J., Napiwotzki, A., Eichler, H. J., and Renger, G. (1991) Two sites of photoinhibition of the electron transfer in oxygen evolving and Tris-treated PS II membrane fragments from spinach. *Photosynth. Res. 27*, 97–108.
64. Barber, J., and De Las Rivas, J. (1993) A functional model for the role of cytochrome b559 in the protection against donor and acceptor side photoinhibition. *Proc. Natl. Acad. Sci. U. S. A. 90*, 10942–10946.
65. Krause, G. H., and Weis, E. (1991) Chlorophyll fluorescence and photosynthesis: the basics. *Annu. Rev. Plant Physiol. Plant Mol. Biol. 42*, 313–349.
66. van Wijk, K. J., Nilsson, L. O., and Styring, S. (1994) Synthesis of reaction-center proteins and reactivation of redox components during repair of photosystem-II after light-induced inactivation. *J. Biol. Chem. 269*, 28382–28392.

BI701913K